IOP PUBLISHING NANOTECHNOLOGY
Nanotechnology **18** (2007) 335605 (5pp) doi:10.1088/0957-4484/18/33/335605

Symmetric organization of self-assembled carbon nitride

Li Yang[1,5], Paul W May[1], Lei Yin[2], Yizhong Huang[3], James A Smith[1] and Tom B Scott[4]

[1] School of Chemistry, University of Bristol, Cantock's Close, Bristol BS8 1TS, UK
[2] Advanced Composites Centre for Innovation and Science (ACCIS), Department of Aerospace Engineering, University of Bristol, Queen's Building, University Walk, Bristol BS8 1TR, UK
[3] Department of Materials, University of Oxford, Oxford OX1 3PH, UK
[4] Interface Analysis Centre, University of Bristol, Oldbury House, 121 St Michael's Hill, Bristol BS2 8BS, UK

E-mail: li.yang@bristol.ac.uk

Received 13 April 2007, in final form 22 June 2007
Published 25 July 2007
Online at stacks.iop.org/Nano/18/335605

Abstract
A scheme for creating 'flower-like' nanostructures of carbon nitride is described that involves the self-assembly of nanocrystals following laser ablation of a solid graphite target immersed in aqueous ammonia solution. The primary nanocrystals possess rod-like symmetry, and then self-assemble upon drying to form nanoleaf or nanopetal shaped structures. Samples were characterized using x-ray diffraction (XRD), transmission electron microscopy (TEM), field-emission scanning electron microscopy (FE-SEM), x-ray photoelectron microscopy (XPS) and Fourier transform infrared spectroscopy (FTIR). The analyses confirmed their composition to be consistent with that of crystalline β-phase carbon nitride. The morphologies of the carbon nitride nanostructures depended strongly on the synthesis conditions and upon the conditions under which the aqueous suspension of ablated particles were dried.

1. Introduction

Although self-assembly has occurred in nature for thousands of years (for instance, the formation of salt crystals and the intricate structure of snowflakes), the term 'self-assembly' as used in chemical synthesis is relative new. Self-assembly refers to the creation, by physical or chemical reaction, of small building units, which may be nanoparticles (NPs), nanorods (NRs), etc, which then aggregate together in specific arrangements to give one-dimensional (1D), two-dimensional (2D) or even three-dimensional (3D) superstructures [1]. The aggregation may be spontaneous without human intervention, or may be as a result of changing local conditions, e.g. temperature, concentration, drying, etc. Current understanding extends only to the most rudimentary of these stages for its use in materials science, biology, chemistry and condensed matter science [2, 3].

In recent years much progress has been made on the preparation of inorganic metals, metal oxides and other semiconductors with a range of morphologies, such as compact hexagonal networks [4], rings [5], dandelion-shaped hollow structures [6], strips [7], tubes [8] and flower-like structures [9]. However, there has been little effort devoted toward the understanding of the self-assembly processes of group IV–V compounds, such as carbon nitride. Although carbon nitride has been the subject of numerous publications since the prediction by Liu and Cohen [10] in 1989 that crystalline C_3N_4 should have super-hard properties, the successful synthesis of bulk amounts of this material still remains a challenge. Recently Li and co-workers [11] demonstrated that a range of self-assembled carbon nitride morphologies (including nanotube bundles, aligned nanoribbons and microspheres) can be prepared by a solvothermal technique. Cao and co-workers [12] reported that carbon nitride nanotubes had been synthesized on a large scale through a catalytic-assembly solvothermal route involving the reaction of cyanuric chloride ($C_3N_3Cl_3$) with sodium, using $NiCl_2$ as a catalyst precursor. Also, our recent findings [13, 14] indicated that by using liquid-phase pulsed laser ablation

[5] Author to whom any correspondence should be addressed.

 © 2007 IOP Publishing Ltd Printed in the UK

(LP-PLA), i.e. where a high-intensity focused laser beam impinges upon a graphite target confined by a thin layer of liquid ammonia solution, a versatile morphology of carbon nitride such as nanospheres, nanoleaves and complex 3D well-arranged architectures can be created. Their structures and spatial organization are controllable by changing the deposition and drying conditions. Concerning the unique properties and new structural features of carbon nitride, it may be of fundamental interest to investigate an underlying process based on morphological control. In particular, new concepts of self-assembly in carbon nitride would be highly desirable.

To date, most reports of nanomaterials made by LP-PLA have been either continuous film structures, zero-dimensional (0D) NPs [15] or 1D NRs [16, 17]. Since the 0D and 1D nanocrystals can serve as building blocks in forming 2D or 3D complex architectures with long range periodic structures, it should be expected that the LP-PLA approach would have great potential as a means to grow large arrays of hierarchical, complex, oriented and ordered superstructures. In this paper we demonstrate a fabrication scheme for free-standing, hierarchical self-assembly of carbon nitride structures from small 0D or 1D building blocks. This approach has involved initially using the LP-PLA process to prepare carbon nitride NP suspensions, and then sequentially seeding these onto an appropriate substrate and carefully drying away the liquid. This approach may be used to generate more complex nanostructures, such as those observed in natural materials or biominerals [18], and be extended to a range of other solid materials, such as zinc oxide [19].

2. Experimental details

The carbon nitride nanocrystal seed solution was prepared by LP-PLA, details of which are given elsewhere [20]. Briefly, a solid graphite target (Testbourne Ltd, 99.99%) was ablated at room temperature while submerged in a 5 ml solution of 25%–35% ammonia solution (Fisher Scientific, used as-received without further purification) inside a sealed stainless steel cell. A Q-switched Nd:YAG laser (532 nm, pulse duration 15 ns, frequency 10 Hz) was directed by a prism and then focused onto the graphite surface using a lens with a focal length of 25 mm. The intense laser light passed through a quartz window in the top of the cell and then through a ∼5 mm layer of the liquid covering the graphite, to form a ∼0.5 mm diameter spot on the target surface. The ablation was typically carried out at laser fluences of 25–125 mJ per pulse for reaction times t = 0.5–12 h. After ablation, a pale yellow colloidal suspension was obtained, which contained a mixture of unreacted graphite and ablation product, both in the form of NPs. The suspension was stable, with no precipitate being observed for months or even longer. The graphite sediments were filtered and removed as much as possible by boiling with 70% perchloric acid, before further characterization.

For materials analysis, the suspension was deposited onto a silicon p-type (100) substrate or TEM grid, and then allowed to dry in air or in a sealed tube. This procedure allowed the time taken to evaporate the liquid to be controlled. The product was characterized using x-ray diffraction (XRD; Bruker-AXS D8 powder diffractometer, Cu Kα radiation), field emission scanning electron microscopy (FE-SEM; JEOL 6300 F), transmission electron microscopy (TEM; JEOL 1200 EX, 120 kV), high-resolution (HR) TEM (JEOL 3000 F, 300 kV) and energy-dispersive x-ray analysis (EDX). X-ray photoelectron spectroscopy (XPS; Thermo VG Scientific), laser Raman spectroscopy (Renishaw 2000, excitation wavelength 325 nm) and Fourier-transform infrared spectroscopy (FTIR; using a KBr disc) were performed to search for evidence of C–N, C=C and C≡N bonds.

3. Results and discussion

All reported samples in the present work were first examined with XRD, EDX, Raman and XPS techniques to obtain their crystallographic structure and chemical composition. Experimental details of the procedures can be seen in our previous reports [13, 18, 20]. These analyses show that the prepared nanocrystals are consistent with hexagonal β-C_3N_4 ($P6_3/m$ (176)) with lattice constants a_0 = 6.4017 Å and c_0 = 2.4041 Å (spectra not shown here) [21]. In particular, the strong (200) reflection from the XRD peaks which have the highest intensity reveals the preferred ⟨100⟩ orientation of the nanocrystallites [18].

The TEM analysis revealed that the ablated carbon nitride structures have a range of unusual morphologies. Since both ends of the flat structures taper to a point, they resemble the shape of a leaf, and so we have termed them 'leaf-like' structures. These nanoleaf structures are generated by the coalescence and self-assembly of 0D (NP) or 1D (NR) building blocks, which organize themselves in different ways. Figure 1 illustrates three types of nanoleaf organization [22]. The first type (I) of organization is based on a large number of 0D NPs close-packed together to form dense leaf-like structures with smooth surfaces (figures 1(a) and (b)). The second type (II) of organization is obtained when long NR (figure 1(c)) or short NR (figure 1(d)) units point in the same direction, and are *parallel* and well-aligned along the propagating long-axis. This forms nanoleaves with a rough, less dense surface, with plenty of voids situated between some of the component nanorods. Although individual leaf-like structures within a local region seem to be randomly oriented, the overall NR aggregates still exhibit long-range ordering. The third type (III) of organization is more rigidly constructed from numerous closely packed NRs. Unlike type (II), however, the NRs are now preferentially aligned *perpendicular* to the long-axis of the leaf-like aggregates (figures 1(e) and (f)). These nanoleaves have a dense, rough surface. However, it should be mentioned that the latter two cases can be treated as an extension of type (I), because these NRs are themselves composed of numerous smaller NPs that have packed together in an ordered arrangement to form rod-like shapes (figures 1(d) and (f)).

The morphology of the self-assembled carbon nitride nanostructures was tuneable with the reaction conditions. By varying the ablation time, laser energy and ammonia concentration, different final complex architectures could be achieved on various length scales. The dependence of the structural morphology and experimental conditions can be seen in our previous reports [13, 18, 20]. In general, the trend is that the size of the overall nanocrystallites and their basic building blocks increases with increasing laser power and the ablation time. Three main classes of structure have

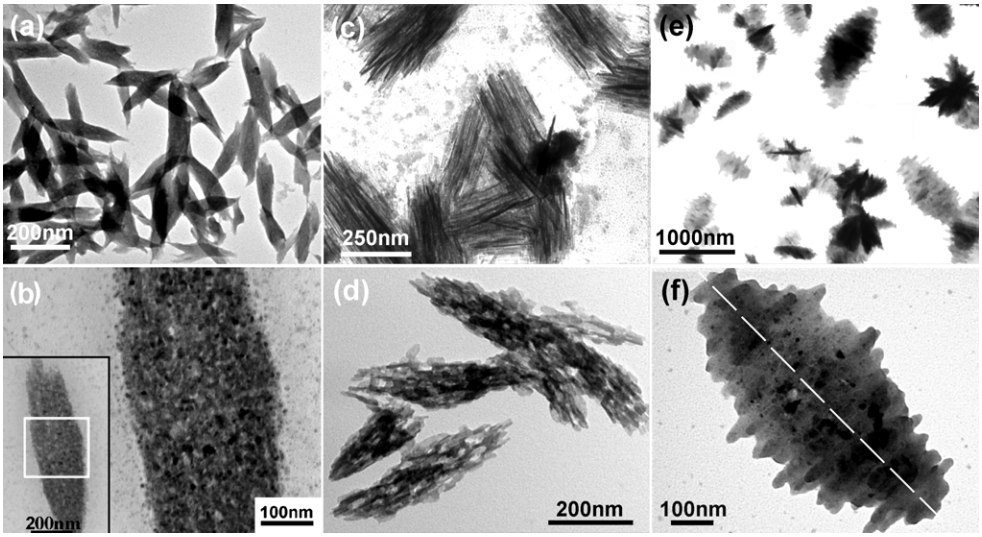

Figure 1. TEM images of ((a), (b)) the type (I) organization to form dense leaf-like carbon nitride structures. (b) A single leaf-like unit formed from numerous small NPs (inset area framed with white box). ((c), (d)) Type (II) organization with the NRs arranged parallel to the long-axis of the nanoleaf. ((e), (f)) Type (III) organization with the NRs arranged perpendicular to the long-axis of the nanoleaf. (f) A single leaf-like type (III) nanocrystallite made from 1D NRs preferentially aligned perpendicular to the long-axis (dashed line).

been identified in the ablation product, categorized based upon their shape (figure 2). The first class of structure had the shape of nearly monodispersed spheres with rounded edges (figure 2(a)). Those spheres have a very high density and are close-packed. The second class of nanostructure resembles 'flower-like' spiked crystallites (figure 2(b)), where the NRs have coalesced at a common centre with multi-fold symmetry. It seems that these flower-like structures are simply less dense versions of the spheres (figure 2(c)), with numerous voids between the NR framework comprising the flowers. Smaller NPs which lie in and around the NR framework appeared to be mobile with respect to this framework, and diffused outward from the centre of the flower with longer drying times. The results of this diffusion can be seen in figure 2(d), where the solid carbon nitride flower (similar to that in figure 2(b)) has become hollow. This produces the third class of nanostructure, which we have called 'hollow-flowers'. In these structures, the NPs have diffused from the centre but remain loosely attached to the outside, making the outer shell of the flower appear fuzzy. It is worth pointing out that by simply altering the drying time and drying method of the suspension, the final morphology can exhibit semi-hollow, core-shell or even full-hollow structures. These observations are similar to the report by Liu and Zeng [23], who demonstrated the fabrication of ZnS nanomaterials with hollow interiors. Yang and Zeng also reported a simple approach to prepare hollow TiO_2 nanospheres with highly organized crystallites in the shell structure and surface regions [24]. Compared to the second class of structure (flower-like), the third class (hollow-flowers) is less common. A longer drying time in an above ambient temperature helps the small crystallites to move freely in the solution enabling oriented aggregation. The ratios of population among the first, second and third classes of structures are approximately 30%, 60% and 10%, respectively (based on a total of 800 TEM images), noting that the statistical ratios vary for different experimental conditions. In general, a higher synthetic energy (i.e. high laser power, long ablation time, high ammonia concentration and long drying time) leads to a better crystallinity but larger size for the products.

In principle, assembly is energetically favoured because the formation of larger crystals can greatly reduce the interfacial energy of isolated NPs or NRs. Therefore, most of our final products are either well-defined leaf-like structures or self-assembled flower-like architectures. Only occasionally were monodispersed NPs or isolated NRs seen in the TEM observations. The mechanism for how these lower dimensional building blocks construct to higher dimensional arrangements, rather than random clumps, is still unclear. However, the above evidence indicates that 'oriented attachment' [25] was observed among the crystallites, in which a larger crystal structure is formed from smaller ones by direct joining of suitable crystal planes. In particular, in the HRTEM image of figure 2(e) taken from a single NR, the periodic lattices show the atomic arrangement (figure 2(e), inset) with very few defects, and reflect the relationship between the orientation of the NPs and the crystallography of the ordered NR array. The corresponding Fourier-filtered transform (FFT) pattern illustrates that the nanocrystal consists of six domains with sixfold twins. The split spots K and J, H and G in the FFT pattern is due to the small angle between the twin boundaries. The reflections P and P′ in figure 2(f) are not split, and represent the coherent positions of the twin boundaries.

The information regarding the chemical bonding structure was obtained from FTIR spectroscopy. Figure 3 shows the FTIR spectra of the above-mentioned three classes of carbon nitride crystals, which exhibit several peaks related to the chemical bonding between carbon and nitrogen [26]. The region 1000–1500 cm^{-1} corresponds to C–N single bonding, while the regions 1500–1750 cm^{-1} and 2150–2300 cm^{-1} are related to C=N and C≡N bonding, respectively. Similar spectra were also obtained by Zimmerman and co-workers [27]. In our case, for nanosphere structures

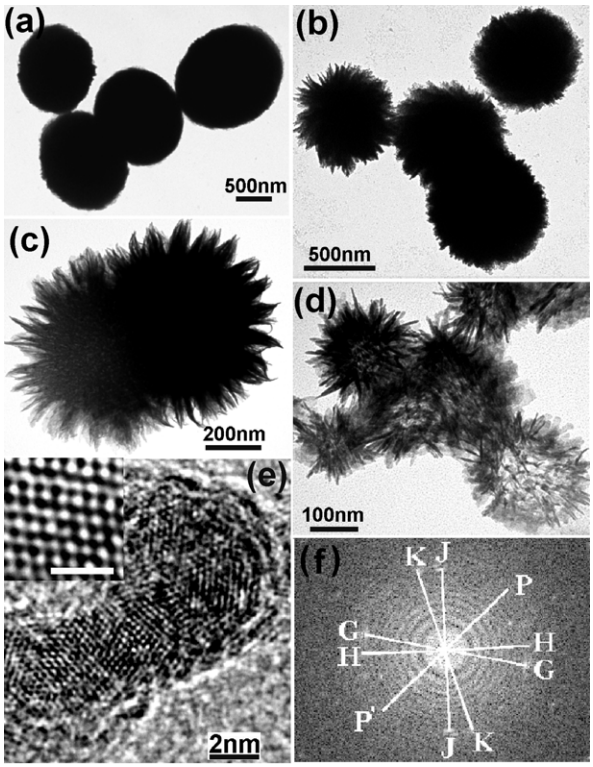

Figure 2. (a) Nanospheres with rounded edges (synthesis conditions: laser power 50 mJ, ablation time 2 h, 35% ammonia solution, drying in air). ((b), (c)) Nanoflowers with numerous protruding spiky surfaces (synthesis conditions: laser power 100 mJ, ablation time 8 h, 35% ammonia solution, drying in air). (d) Hollow-flowers with tunnels connecting from the centre to the outward shell (synthesis conditions: laser power 100 mJ, ablation time 10 h, 35% ammonia solution, drying in a sealed tube). (e) HR-TEM image of a single NR; the inset shows the atomic arrangement and scale bar of 1 nm. (f) The Fourier-filtered transform (FFT) pattern corresponding to the region shown in (e). K, J, H, G, P and P′ label the positions of the six domains (see text for details).

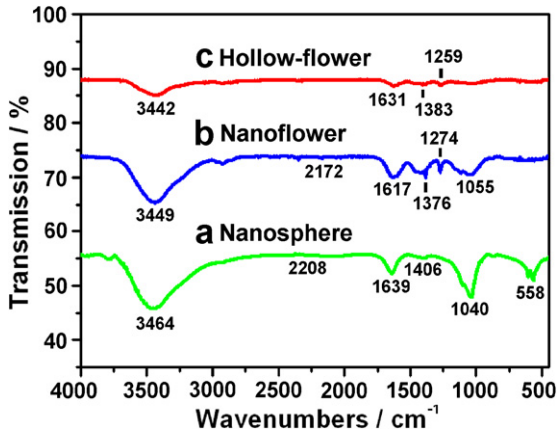

Figure 3. FTIR spectra of the three classes of carbon nitride structures: (a) nanosphere, (b) nanoflower, (c) hollow-flower. (This figure is in colour only in the electronic version)

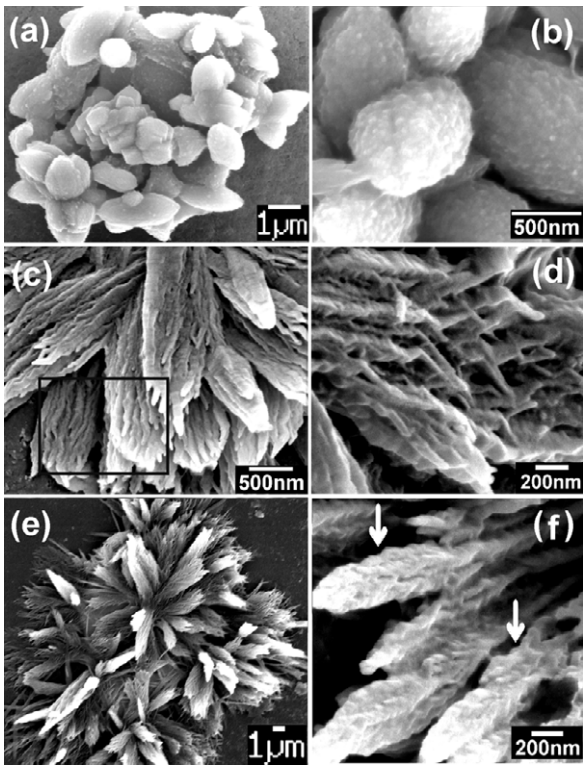

Figure 4. SEM images of (a) nanoleaf aggregates (sample conditions identical to that in figure 1(a)). (b) 3D leaf-like crystals with apparent NPs close-packed on the surface. (c) Leaf-like structures consisting of vertical NR branches (region highlighted by black box). (d) Interwoven NR arrangements to construct the final superstructures. (e) An individual flower exhibiting multi-fold symmetry. (f) The assembly of higher-order nanopetal structures constructed by numerous subunits. Arrows highlight NPs close-packed onto the wall, making the nanopetal surface rough and curved.

(figure 3(a)) the two peaks at 1040 and 1406 cm^{-1} correspond to the C–N stretching mode. The absorption band at 1639 cm^{-1} is assigned to the stretching vibrational modes of the C=N. Moreover, a small peak at 2208 cm^{-1} can probably be attributed to C≡N bonds, although it is much weaker than the other stretching modes. A broad band centred at 3464 cm^{-1} is due to NH group vibrations [28]. The 558 cm^{-1} peak can be assigned to the out-of-plane bending mode for graphite-like sp^2 domains, which become IR active due to nitrogen incorporation into the bonding network. The obvious differences between these samples are that the intensities of all the features are weaker and broader for the nanoflower and hollow-flower shape nanostructures. We attributed this to the voids in the nanoflowers and the internal nanospaces existing in the hollow-flowers.

More images of the symmetric organization can be obtained by FE-SEM analysis, as shown in figure 4. By controlling the drying time, the different types of organization mentioned previously can be obtained when the carbon nitride colloid produced in the initial LP-PLA step was physically deposited onto a Si wafer. Figures 4(a) and (b) (sample synthesis conditions identical to those for figure 1(a)) give further evidence for type (I) organization, i.e. the NPs have attached side-by-side and have fused into the surface of the leaf-like structures (figure 4(b)). Such arrangements were observed following a very quick drying process, for example

drying in an oven or on a hotplate in less than an hour. In contrast, if the substrate was dried in air or inside a sealed tube (water evaporation time ∼8 h or longer), the individual NRs assembled vertically into bundles (see the highlighted box region in figure 4(c)) and formed leaf-like structures. Surprisingly, when the evaporation time of the liquid was increased to 12 h, these NRs appeared to be 'interwoven' together into a lattice-like framework (figure 4(d))—yet the NRs were still aligned along the *c*-axis direction of the final complex architectures. These structures can be assigned as type (II), mentioned previously. A possible explanation is that the longer time for evaporation of the liquid allows sufficient time for the diffusion of all the NPs out of the flowers, leaving some liquid trapped into the gaps between the NR framework. The wet NR framework now has the opportunity to recrystallize or restructure into the shapes shown in figure 4(e). It was found that this mesophase flower has a symmetric structure consisting of many 2D radial 'nanopetals' (named since they were the components of the larger flower-like structures) and radial growth from a central nucleus [29]. In addition, each nanopetal is constructed from many tiny nanocrystals or NR subunits (figure 4(f)), as seen at the edge of the nanopetals. Those smaller NPs close-packed onto the wall of the nanopetals, making the nanopetal surface rough and curved (highlighted by arrows in figure 4(f)). New nanocrystals then nucleate on the existing crystals and share the same edges. It is worth pointing out that the length of the nanopetals is in the range of 1–20 μm, while the sizes of the subunit NPs (5–20 nm) or NRs with a rod diameter of 10–20 nm have barely changed. It seems that the solid Si substrate aids the initial self-assembly. That is, the presence of the substrate physically hinders growth in that direction; so many nanopetal branches are tilted away from the substrate. These structures are close-packed but still have spaces between them. The excess vacancies between the nanocrystals are favourable sites to be filled up by the continuous flux of particles, which is accomplished by consequental atom to atom lining up to reorganize and crystallize the well-defined 3D complex shapes mentioned in figure 4(e).

4. Conclusions

In summary, a simple scheme for the construction of self-assembled carbon nitride complex structures has been elucidated by LP-PLA using solid graphite and ammonia solution: (1) formation of 1D NRs from smaller 0D NPs via oriented aggregation and (2) arrangement of these units into 2D carbon nitride nanoleaves or 3D nanoflowers. A key advantage afforded by this approach is the ability to systematically generate and control a diverse array of structures from a simple and inexpensive chemical route. Such controllable morphology would give carbon nitride potential applications in micro- and nanomechanics, microlevers and tips for scanning probe microscopes, etc. Further investigation of the mechanical properties is required to ascertain if nanophase carbon nitride has the required hardness and wear resistance for these applications. This self-assembly concept may be extended to prepare other metals, metal oxides and covalent compound materials. With this improved understanding, LP-PLA may provide a versatile and powerful industrial scale production process for assembling complex architectures by specific design.

Acknowledgments

This work was supported by Universities UK via the Overseas Research Scholarship (ORS) scheme and the University of Bristol. The authors are very grateful to Dr S A Davis, J Jones, K N Rosser, C Archer and R Brown for their many and varied contributions to the work described herein.

References

[1] Whitesides G M and Grzybowski B 2002 *Science* **295** 2418
[2] Whitesides G M and Boncheva M 2002 *Proc. Natl Acad. Sci. USA* **99** 4769
[3] Su W T, Li B, Yin L, Yang L, Liu D Q and Zhang F S 2007 *Appl. Surf. Sci.* **253** 6259
[4] Motte L, Billoudet F and Pileni M P 1995 *J. Phys. Chem.* **99** 16425
[5] Maillard M, Motte L and Pileni M P 2001 *Adv. Mater.* **13** 200
[6] Liu B and Zeng H C 2004 *J. Am. Chem. Soc.* **126** 16744
[7] Petit C, Legrand J, Russier V and Pileni M P 2002 *J. Appl. Phys.* **91** 1502
[8] Ngo A T and Pileni M P 2000 *Adv. Mater.* **12** 276
[9] Liu J P, Huang X T, Li Y Y, Sulieman K M, He X and Sun F L 2006 *J. Mater. Chem.* **16** 4427
[10] Liu A Y and Cohen M 1989 *Science* **245** 841
[11] Li J, Cao C B, Hao J W, Qiu H L, Xu Y J and Zhu H S 2006 *Diamond Relat. Mater.* **15** 1593
[12] Cao C B, Huang F L, Cao C T, Li J and Zhu H S 2004 *Chem. Mater.* **16** 5213
[13] Yang L, May P W, Yin L, Brown R and Scott T B 2006 *Chem. Mater.* **18** 5058
[14] Yang L, May P W, Yin L, Smith J A and Rosser K N 2007 *J. Nanopart. Res.* at press doi:10.1007/s11051-006-9192-4
[15] Yang L, May P W, Yin L, Smith J A and Rosser K N 2007 *Diamond Relat. Mater.* **16** 725
[16] Nath M, Rao C N R, Popvitz-biro R, Albu-Yaron A and Tenne R 2004 *Chem. Mater.* **16** 2238
[17] Liang C H, Sasaki T, Shimizu Y and Koshizaki N 2004 *Chem. Phys. Lett.* **389** 58
[18] Yang L, May P W, Huang Y Z and Yin L 2007 *J. Mater. Chem.* **17** 1255
[19] Yang L, May P W, Yin L and Scott T B 2007 *Nanotechnology* **18** 215602
[20] Yang L, May P W, Yin L, Scott T B, Smith J A and Rosser K N 2006 *Nanotechnology* **17** 5798
[21] Wang J, Lei J and Wang R 1998 *Phys. Rev.* B **58** 11890
[22] Liu B and Zeng H C 2005 *J. Am. Chem. Soc.* **127** 18262
[23] Liu B and Zeng H C 2005 *Small* **1** 566
[24] Yang H G and Zeng H C 2004 *J. Phys. Chem.* B **108** 3492
[25] Penn R L and Banfield J F 1998 *Science* **281** 969
[26] Lu T R, Kuo C T, Yang J R, Chen L C, Chen K H and Chen T M 1999 *Surf. Coat. Technol.* **115** 116
[27] Zimmerman J L, Williams R, Khabashesku V N and Margrave J L 2001 *Nano Lett.* **1** 731
[28] Likhacheva A Y, Paukshtis E A, Seryotkin Y V and Shulgenko S G 2002 *Phys. Chem. Miner.* **29** 617
[29] Li Z Q, Xiong Y J and Xie Y 2005 *Nanotechnology* **16** 2303